Biochimica et Biophysica Acta 1818 (2012) 889–895

Contents lists available at SciVerse ScienceDirect

Biochimica et Biophysica Acta

journal homepage: www.elsevier.com/locate/bbamem

Transmembrane and extramembrane contributions to membrane protein thermal stability: Studies with the NaChBac sodium channel

Andrew M. Powl, Andrew J. Miles, B.A. Wallace *

Department of Crystallography, Institute of Structural and Molecular Biology, Birkbeck College, University of London, London WC1E 7HX, UK

ARTICLE INFO

Article history:
Received 10 August 2011
Received in revised form 30 November 2011
Accepted 20 December 2011
Available online 29 December 2011

Keywords:
Protein stability
Membrane protein folding/unfolding
Synchrotron radiation circular dichroism (SRCD) spectroscopy
Secondary structure
Extramembrane and transmembrane domains

ABSTRACT

The thermal stabilities of the extramembranous and transmembranous regions of the bacterial voltage-gated sodium channel NaChBac have been characterised using thermal-melt synchrotron radiation circular dichroism (SRCD) spectroscopy. A series of constructs, ranging from the full-length protein containing both the C-terminal cytoplasmic and the transmembranous domains, to proteins with decreasing amounts of the cytoplasmic domain, were examined in order to separately define the roles of these two types of domains in the stability and processes of unfolding of a membrane protein. The sensitivity of the SRCD measurements over a wide range of wavelengths and temperatures has meant that subtle but reproducible conformational changes could be detected with accuracy. The residues in the C-terminal extramembranous domain were highly susceptible to thermal denaturation, but for the most part the transmembrane residues were not thermally-labile and retained their helical character even at very elevated temperatures. The process of thermal unfolding involved an initial irreversible unfolding of the highly labile distal extramembranous C-terminal helical region, which was accompanied by a reversible unfolding of a small number of helical residues in the transmembrane domain. This was then followed by the irreversible unfolding of a limited number of additional transmembrane helical residues at greatly elevated temperatures. Hence this study has been able to determine the different contributions and roles of the transmembrane and extramembrane residues in the processes of thermal denaturation of this multipass integral membrane protein.

1. Introduction

Soluble proteins have been well characterised with respect to their unfolding/folding processes, thermal stabilities, and folding intermediates [1,2]. However, by comparison, relatively few studies have characterised the processes of unfolding and folding in membrane proteins. This is, in part, due to the challenge of obtaining accurate measurements on these scarce molecules with limited solubilities, the necessity of using detergent or lipid molecules to maintain their solubility, and also because of the difficulty in interpreting the convoluted effects present in multi-domain proteins (i.e. ones with both transmembrane (TM) and extramembrane (EM) regions).

As with studies on soluble proteins, membrane proteins can be denatured by both physical and chemical methods in order to gain insight into the mechanisms and thermodynamics of unfolding, as well as to provide information on the structure of the denatured protein [3]. Physical methods for unfolding include heat treatment [4,5], pressure [6], and dynamic force microscopy [7], whilst chemical denaturants [8] include guanidine hydrochloride, urea, the ionic detergent sodium dodecyl sulfate (SDS), and organic solvents [9]. Each denaturation method used to probe protein stability has its own set of advantages and limitations. Physical denaturation by heat treatment is advantageous in that it generally does not alter other properties of the solution such as ionic strength and does not require the presence of any denaturing chemical that itself can interfere with spectroscopic measurements. However, as with other techniques, it can result in irreversibly aggregated samples, and hence, may only permit qualitative interpretations rather than determination of thermodynamic parameters. Pressure denaturation can be difficult to control and may result from indirect effects on the lipid components [10]. Dynamic force measurements mostly provide information on the process of membrane protein interactions with bilayers rather than the unfolding process itself [11]. Chemical denaturations using guanidine hydrochloride or urea tend to only be effective at very high concentrations (near their solubility limits) and often do not significantly denature transmembrane α-helices as they tend to localise and act primarily in the EM region [12]. Organic solvents have converse limitations as they tend to partition preferentially

Abbreviations: CD, circular dichroism; Cymal-5, 5-cyclohexyl-1-pentyl-β-D maltoside; EM, extramembrane; FL, full-length (native) NaChBac; NaChBac, voltage-gated sodium channel from *B. halodurans*; SDS, sodium dodecyl sulfate; SRCD, synchrotron radiation circular dichroism; TM, transmembrane; VGSC, voltage-gated sodium channel

* Corresponding author. Tel.: +44 207 631 6800; fax: +44 207 631 6803.
E-mail address: b.wallace@mail.cryst.bbk.ac.uk (B.A. Wallace).

0005-2736/$ – see front matter © 2011 Elsevier B.V. All rights reserved.
doi:10.1016/j.bbamem.2011.12.019

into the membrane region [13], can be volatile and thus lost during the unfolding process, and some such as trifluoroethanol tend to induce helical structures rather than unfold them [9]. SDS has the advantage of being effective at millimolar concentrations and able to form mixed micelles with other detergents, but this denaturant often results in only partial unfolding of membrane proteins, and because it tends to induce helical structures, can result in "denatured" proteins with non-native helical structure [14]; indeed even β-pleated sheets can be transformed into α-helical structures in the presence of "denaturing" concentrations of SDS [15].

Overall, membrane proteins appear to be much more resistant to both chemical and thermal denaturation than are soluble proteins [16–18], with significant amounts of their secondary structures remaining even after extensive thermal or chemical treatment [8]. It has been suggested that the EM regions of the protein may be more susceptible to unfolding whilst the TM domains retain much of their native structure under various denaturing conditions [19], but there have been few studies defining the relative contributions of the extramembranous and transmembranous domains and the roles of different types of secondary structures in each of these regions in maintaining protein stability.

A very useful system for investigating the nature of unfolding in a multidomain membrane protein is the voltage-gated sodium channel (VGSC) from *Bacillus halodurans* (NaChBac). Bacterial sodium channels are tetrameric and hydropathy plots predict that all bacterial sodium channel monomers possess the same structural motif of six TM segments in addition to an extended cytoplasmically-exposed C-terminal domain (CTD) [20] (Fig. 1). In recent studies it was shown that the CTD of NaChBac is not required for tetramer formation [21], but may be important for initial assembly in membranes [22]. The structure of the C-terminal domain of NaChBac has been shown experimentally [22] to consist of a proximal unstructured region, which is followed by a distal helical structure.

In this study, we have produced both full length (FL) NaChBac and a series of C-terminally truncated constructs in order to separately dissect the thermal stabilities of the TM and EM regions, and to identify the different contributions of helical and unstructured residues in the EM domain to the thermal stability and unfolding processes. The highly sensitive method of synchrotron radiation circular dichroism (SRCD) spectroscopy was used to monitor and quantify relatively subtle changes in the secondary structure of FL NaChBac and the truncated constructs as a function of temperature, and to identify the pathways involved in its unfolding and refolding.

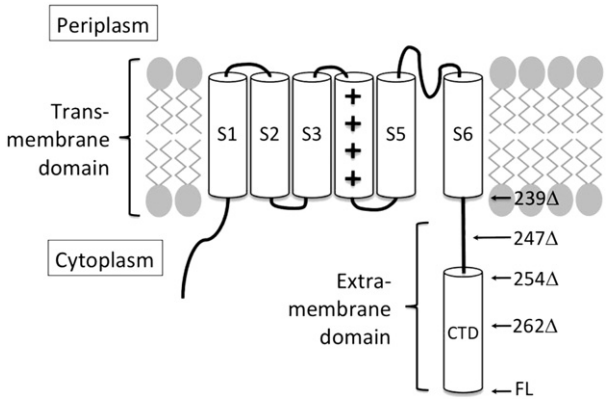

Fig. 1. Topology model of NaChBac, with the helical six transmembrane segments (S1 to S6) and the helical C-terminal domain (CTD) shown as cylinders. The sites of truncation of the various constructs (designated by the number of the first residue removed, with FL meaning full-length) are indicated by black arrows.

2. Materials and methods

2.1. Materials

The cDNA for NaChBac was provided by Prof. David Clapham of Harvard Medical School. N-dodecyl-β-D maltopyranoside and 5-cyclohexyl-1-pentyl-β-D maltoside (Cymal-5) were obtained from Anatrace. All other reagents were purchased from Sigma, unless otherwise stated.

2.2. Expression and purification

C-terminal truncated NaChBac constructs were generated using the QuikChange protocol from Stratagene to introduce stop codons into the full-length *NaChBac* cDNA as described in Powl et al. (2010) [22]. Protein samples were purified from *E. coli* C41(DE3) cells as described previously [22]. Their purity was assessed by solubilising the samples in NuPAGE lithium dodecyl sulfate sample buffer, followed by sodium dodecyl sulfate-polyacrylamide gel electrophoresis (NuPAGE 4–12% gradient Bis-Tris gel with MOPS). BenchMark molecular mass standards (Invitrogen) were used to calibrate protein molecular weights.

2.3. Synchotron radiation circular dichroism spectroscopy

Protein concentrations were determined immediately prior to measurement of the SRCD spectra using an extinction coefficient at 280 nm calculated from the amino acid sequence using Expasy ProtParam [23] and the A_{280} measured on a Nanodrop 1000 UV spectrophotometer.

SRCD measurements were undertaken on beamline CD1 at the ISA Synchrotron located at the University of Aarhus, Denmark, on beamline 4B8 at the Beijing Synchrotron Radiation Facility (BSRF) in China, and on the DISCO beamline at the Soleil Synchrotron, France. The beamlines were calibrated with camphorsulfonic acid at the beginning of each data collection run. Samples at concentrations of ~4 mg/ml in 50 mM NaCl, 20 mM sodium phosphate, pH 7.8, 0.3% Cymal-5 containing 10% v/v glycerol were loaded into a quartz Suprasil demountable cell (Hellma UK Ltd) with a pathlength of 0.0015 cm. On beamline CD1, SRCD spectra were measured over the wavelength range from 260 nm to 180 nm with a step size of 1 nm and a dwell time of 2 s. Three replicate scans were measured at each temperature between 20 °C and 85 °C. The temperature was raised in 5 °C increments allowing 3 min for the temperature to equilibrate prior to data collection. The actual temperature (as opposed to the set temperature) was determined from calibration curve measured using a thermistor probe inside a sample cell containing water. The first and third scans were compared to ensure that the sample had reached equilibrium before the measurements were made. Conditions and parameters on beamline 4B8 were identical except that the equilibration time was 5 min. Replicate scans were averaged and an averaged baseline (obtained using detergent-containing buffer without protein present) was subtracted. The spectra were smoothed with a Savitsky–Golay filter, and scaled to delta epsilon values with the CDTool software [24] using mean residue weight values of 114.4, 114.5, 114.4, 115.0, and 114.9 for the full-length and 262Δ, 254Δ, 247Δ and 239Δ mutants, respectively. Thermal denaturation curves were obtained from the delta epsilon values for each of the three peaks (222 nm, 209 nm and 192 nm) at each temperature; they were normalised by setting the peak values at 20 °C to 1.0. The data points were fitted with Boltzman functions in Origin (version 8.0).

2.4. Secondary structure analyses

Secondary structure analyses based on SRCD data were carried out using the DichroWeb analysis server [25]. Values reported are the

averages obtained from the ContinLL [26,27], Selcon3 and CDSSTR [28] algorithms (using the SP175t reference dataset [29]).

Principal component analyses were undertaken using the Csel2 algorithm implemented in CDtools [24], which is based on the singular value deconvolution method of Hennessey and Johnson [30].

Secondary structure analyses based the crystal structure of the NavAb homologue (PDB code 3RVY) [31] were undertaken using the DSSP algorithm [32] as implemented in the 2Struc server [33]. The number of helical residues observable in the crystal structure was 181 out of the total of 267 residues present in the protein.

2.5. Data sharing

The spectra and metadata for the thermal melt studies on the FL, 254Δ, and 239Δ constructs have been deposited in the Protein Circular Dichroism Data Bank [34] (located at http://pcddb.cryst.bbk.ac.uk) with the accession codes: CD0001109000 to CD0001111014 for release upon publication.

2.6. Size exclusion chromatography

The longest (full length) and shortest (239Δ) protein constructs (at 5 mg/ml) were split into three equal portions, each containing 1 mg of protein in 50 mM NaCl, 20 mM sodium phosphate, pH 7.8, 0.3% Cymal-5 containing 10% v/v glycerol. Each sample was then heated to either 25°, 50° or 75 °C using the same temperature protocol used in the SRCD measurements. The samples were loaded onto a size-exclusion column (Superdex 200 10/300; GE Healthcare) equilibrated with 50 mM NaCl, 20 mM sodium phosphate, pH 7.8, 0.3% Cymal-5 containing 10% v/v glycerol at 22 °C and eluted at a rate of 0.5 ml/min; the A_{280} was monitored as a function of elution volume. The column had been calibrated with thyroglobulin, ferritin, amylase, aldolase, alcohol dehydrogenase, conalbumin, ovalbumin, carbonic anhydrase and cytochrome c (from Sigma Aldrich).

3. Results

3.1. Secondary structures of native NaChBac and constructs

In addition to the six transmembrane helices that make up the voltage sensor and pore regions of the bacterial sodium channel NaChBac, this membrane protein has been shown [22] to possesses a cytoplasmically-localised C-terminal domain consisting of 36 residues which extends beyond the membrane (Fig. 1), and which accounts for much of the EM content of the protein (Supplemental Table 1). The sequence of the distal helical residues in the CTD contains a leucine-zipper motif [21,22] hence it has been proposed to form a four-helix coiled-coil structure, similar to the one present in KcsA [35]. The relatively short N-terminal extramembranous region is also predicted to be partially helical (Supplemental Table 2), but there is no experimental evidence for its structure. Most of the EM loop regions are very short and predicted to be unstructured (Supplemental Table 2). NaChBac is also a particularly favourable system for studying the contributions of TM and EM domains because the CTD does not include any aromatic residues, which simplifies spectroscopic interpretation and analyses, and the removal of some or all of the CTD residues does not appear to influence the structure of the remainder of the protein [22].

A series of C-terminal deletion constructs and FL NaChBac were readily expressed and purified (Fig. 2) and shown to be tetrameric in the detergent Cymal-5 (Supplemental Fig. 1). In this study, synchrotron radiation circular dichroism spectroscopy was used, as opposed to conventional circular dichroism (CD) spectroscopy, to characterise the secondary structure and unfolding process because it provides the high levels of sensitivity and accuracy necessary to enable the discernment of small structural differences between closely related NaChBac constructs [22,36].

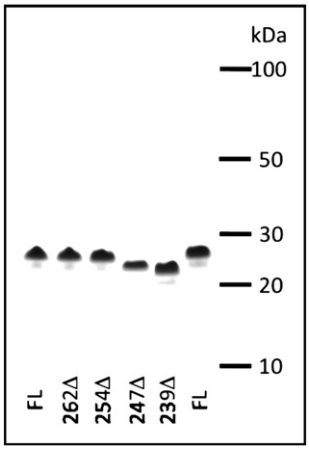

Fig. 2. Coomassie blue stained sodium dodecyl sulfate-polyacrylamide gel electrophoresis of the NaChBac protein constructs. The naming is the same as in Fig. 1.

The SRCD spectra of all the NaChBac constructs at 20 °C (Fig. 3, thick solid lines) exhibit negative peaks at 222 and 209 nm and large positive peaks at 192 nm, indicative of proteins that are both folded and mostly α-helical. The secondary structure of the FL (274 residues)

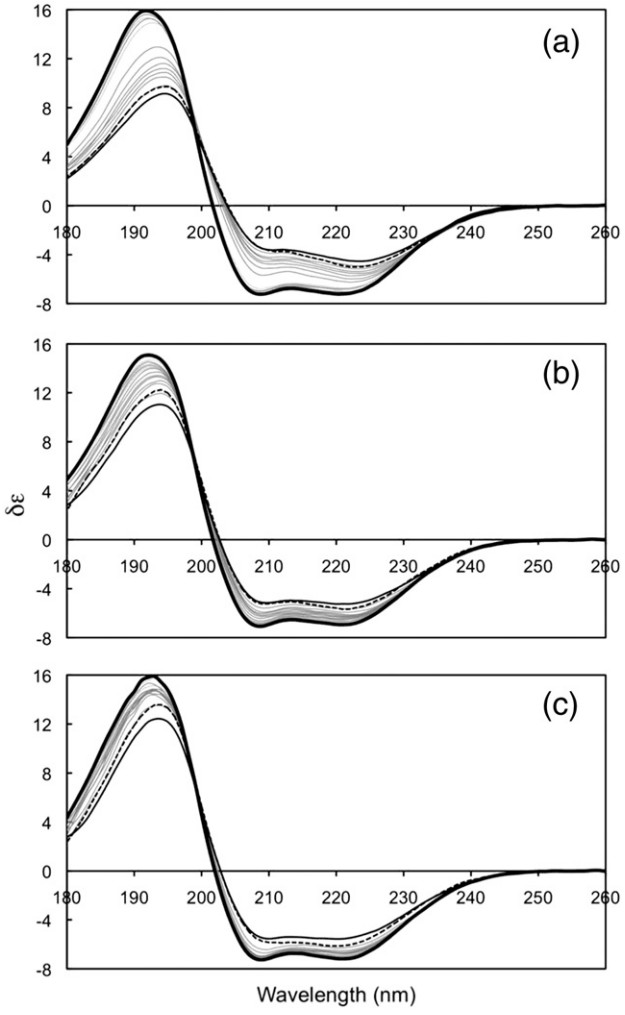

Fig. 3. Synchrotron radiation circular dichroism (SRCD) spectra of NaChBac protein constructs in the detergent Cymal-5 as a function of increasing temperature: 20 °C (thick solid line) to 78 °C (thin solid line) in 5 °C steps (intermediate grey lines), and after cooling from 78° to 20 °C (dashed line) for: (a) FL, (b) 254Δ, and (c) 239Δ constructs.

NaChBac construct, as determined from its SRCD spectrum, is 66% helix and 20% unstructured (Table 1), which is similar to the secondary structure previously determined for this protein in another detergent (dodecyl maltoside) [37]. There are small but significant differences in the spectra of the different NaChBac constructs resulting in differences in their calculated helical content as the CTD is truncated (Table 1). SRCD spectroscopy has provided a complete description of all of the residues in this domain (Supplemental Table 1): The 14 "proximal" residues closest to the end of the S6 helix (i.e. just beyond residue 239) do not adopt regular structures. The 22 distal residues, extending from residue 253 to the C-terminus (residue 274) are all helical in nature (Supplemental Table 1) as predicted (Supplemental Table 2). Hence, the CTD of the FL protein has 22 helical and 14 non-helical residues, construct 262Δ has 9 helical and 14 non-helical, 254Δ has 1 helical and 14 non-helical, 247Δ has 8 non-helical and 239Δ has no CTD residues.

3.2. Thermal unfolding

The thermal stabilities of the NaChBac constructs were assessed by monitoring their far-UV/vacuum-UV SRCD spectra (Fig. 3). The patterns of denaturation seen in the series of spectra obtained for the various constructs are clearly very different, with the FL (Fig. 3(a)) undergoing major changes in magnitude and shape as the temperature is increased above 40 °C. At the highest temperature, not only were all of its peaks decreased in magnitude, but the ratio of its 192 to 222 nm peaks was decreased from 2.19 to 2.03, indicative of a loss of helical structure and a gain in unordered structure. In contrast, the 239Δ construct (Fig. 3(c)), which had no EM CTD, exhibited little change as a function of temperature, with only small differences in magnitudes and ratios (the latter from 2.21 to 2.18), suggesting minimal unfolding of its secondary structure even at the highest temperature. The intermediate constructs (Fig. 3(b)) and data not shown) showed intermediate patterns of unfolding. Taken together these spectra suggest that either the EM CTD itself is more thermally-labile, or else its presence confers lability on the TM domains.

That the primary effect arises from the CTD being more thermally labile than the EM domain is demonstrated from difference curves: Thermal denaturation curves were derived from the magnitudes of the spectra at 192 nm, 209 nm and 222 nm (curves of the 209 nm values for all the constructs are shown in Fig. 4(a)). For each construct (other than 239Δ) the data above 40 °C can be best fit with multi-parameter plots, with the major transition apparently taking place at in the range of 40–50°C and a minor transition with a T_m ~75°C. In the case of 239Δ, only the single transition with the high T_m is evident. If the plot of the 239Δ construct is subtracted from that of the FL construct, this effectively produces the melt curve of the CTD (Fig. 4(b)). The net curve of the CTD can been fit by a single Boltzman curve with a T_m of 46.5°C. The FL melt curve can then be fit by two Boltzman curves, the low temperature CTD curve which accounts for 0.35/0.55 [magnitude of CTD change/magnitude of total change] of the transition and the high temperature curve due to the EM domain, with a T_m of 77.5°C, which accounts for 0.20/0.55 of the change. Once the entire CTD is removed, the overall thermal stability increases dramatically, with only the higher temperature transition present. This suggests that the observed multiphase curves of the various constructs arise from a low temperature unfolding of the CTD followed by an unfolding of the TM domain at a much higher temperature. This demonstrates that the EM region is very much less thermally stable than is the TM domain in all of the constructs, but its presence has little effect on the overall stability of the protein. The singular value deconvolution (SVD) analyses (Fig. 5) showed that for each construct all the unfolding data could be accounted for by two principal components: a helical component which dominates but which diminishes with increasing temperature, and an unordered component which increases with temperature (Fig. 6).

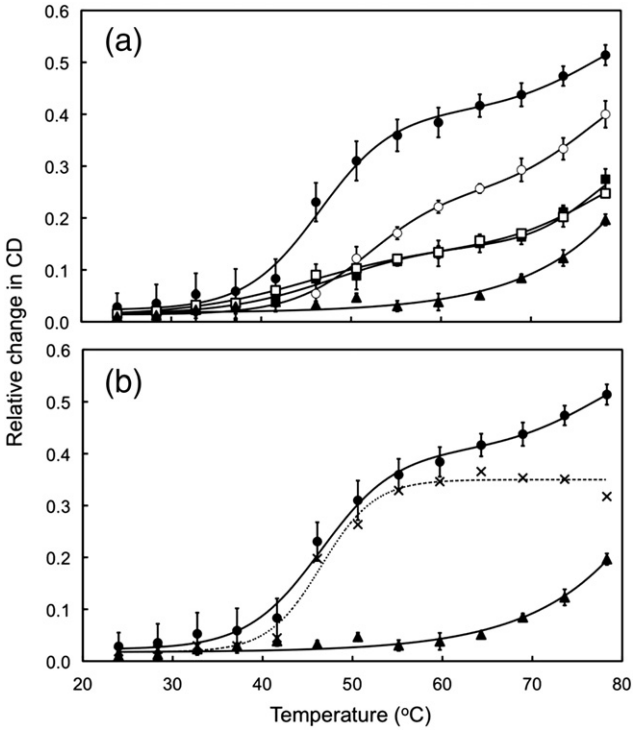

Fig. 4. Thermal denaturation plots (monitoring changes in the magnitude of the 209 nm peak) of: FL (●), 262Δ (○), 254Δ (■), 247Δ (□), and 239Δ 1812 (▲) constructs. (a) original data for all constructs and (b) FL spectrum (●) minus 239Δ (▲) spectrum, producing the net curve for the CTD (X). The error bars represent 1 standard deviation in the measurements between replicate experiments. The fits to the data were produced using Origin v8.0.

Table 1
Secondary structure analyses of each construct at 20 °C and 78 °C and the differences (δ) in secondary structure calculated for each construct at the two temperatures. The values reported are the average results obtained from three different algorithms for two replicate experiments. The ± values listed represent one standard deviation between the 6 analyses obtained for each sample.

Construct/temperature	% helix	No. helical residues lost	No. helical TM residues lost (total-CTD)
FL 20 °C	66 ± 2		
FL 78 °C	42 ± 3		
δ	−24	66	66–22 = 44
262Δ 20 °C	64 ± 2		
262Δ 78 °C	47 ± 3		
δ	−17	45	45–12 = 33
254Δ 20 °C	63 ± 1		
254Δ 78 °C	51 ± 2		
δ	−12	30	30–0 = 30
247Δ 20 °C	64 ± 2		
247Δ 78 °C	53 ± 3		
δ	−11	27	27–0 = 27
239Δ 20 °C	66 ± 2		
239Δ 78 °C	55 ± 3		
δ	−11	26	26–0 = 26

3.3. Secondary structures of unfolded constructs

Comparisons of the calculated secondary structures at 20° and 78 °C (Table 1) indicate some loss of helix occurs for the all constructs at the high temperature, although they still retained a substantial helical content at 78 °C. The results correspond to a minimum of ~120 helical residues retained in all unfolded constructs. This is similar to

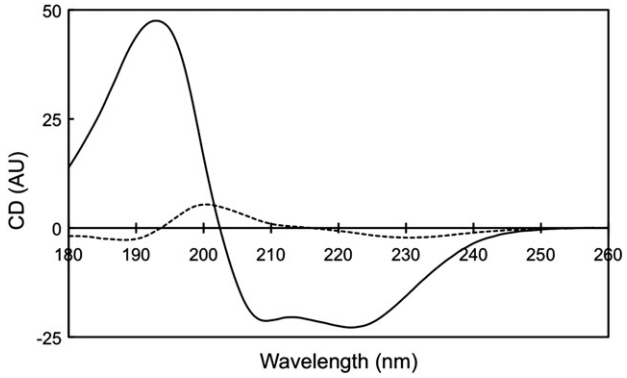

Fig. 5. First (solid line) and second (dashed line) basis spectra for FL protein obtained by singular value deconvolution (SVD) analyses derived from all the SRCD spectra obtained during a thermal melt. The first basis spectrum has the appearance of a classical alpha helix spectrum whereas the second component resembles spectra containing mixed strand and unordered structures. SVD analyses of all of the other constructs produced similar basis spectra, which were then used for the analyses in Fig. 6.

results obtained for sodium channels from other bacterial [38] and eukaryotic [39] sources.

Perhaps more interesting was the observation that there was a subtle decrease in the amount of helix lost at the highest temperatures as the CTD was truncated (Table 1): the 24% lost in the FL protein corresponds to 66 residues. If we assume that 22 of the 66 helical residues lost in the FL come from the CTD, then the number of helical residues lost in the TM domain that accounts for the remainder of the protein would be 44, which again suggests the net unfolding of the TM region is small. For all the other constructs, approximately 30 (± 3) TM helical residues were lost (Table 1). The consistency and magnitude of the number of residues altered in the various constructs (other than FL) suggests that the nature of the change arising from the second (higher) transition could derive from some or all of the following possibilities: 1) the EM N-terminal and loop helical residues (predicted to number around 30–40 (Supplemental Table 2), but for which there is no experimental evidence) also underwent unfolding, 2) one entire TM helix unfolded completely, 3) on average ~2–3 residues at the ends of each of the 6 TM helices unfolded whilst the bulk of the TM region retained its secondary structure integrity, or 4) the final structure is a mixture of folded and slightly unfolded structures (possibly in equilibrium). That the FL protein exhibited more unfolding than the other

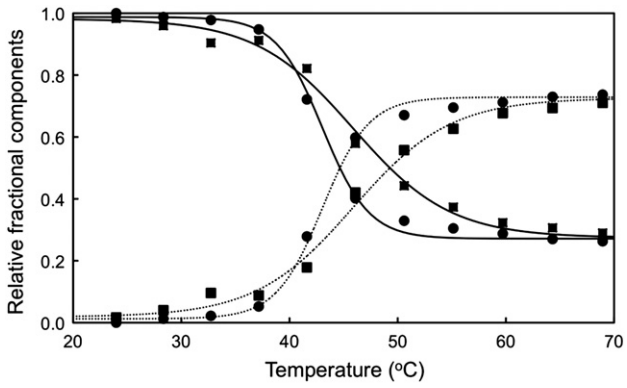

Fig. 6. The fractions of the first (solid line) and second (dashed line) basis spectra that contribute to each SRCD spectrum obtained during a thermal melt as a function of temperature for FL (●) and 254Δ (■) constructs. The curves have been normalised so that the highest value for the first component is 1.0 and the lowest value for the second component is zero. The curves for the 262Δ and 247Δ constructs were intermediate to the ones shown and not included for clarity.

constructs could be due to an extended unfolded CTD interacting with and destabilizing adjacent cytoplasmic EM regions [22]. Hence, these results seem to suggest that the presence of the full CTD imparts enhanced lability on the whole protein, but that once it is no longer intact (perhaps because removal of the distal residues interferes with the four helix leucine zipper), removal of additional amino acids do not alter appear to influence the stability of the remaining TM helical core.

All of the unfolding that occurred when the samples were heated to 78 °C was irreversible; cooling the samples from 78° to 20 °C did not reproduce the original spectra (Fig. 3). Indeed the 192-to-222 nm peak ratio decreased even further (to 1.95) for the FL protein (Fig. 3(a)), suggesting that the unfolded proteins aggregated during the cooling process, with no indication of an increase in 222 nm peak that would be associated with regaining of helical residues, nor any increase in the derived helical secondary structural content. The spectrum of the shortest construct (239Δ (Fig. 3(c)) did not change very much between the low and high temperatures; however, part (but not all) of the helical content was regained upon cooling. The cooled spectra of the intermediate constructs more closely resembled the case of the FL protein in that they did not recover substantially upon cooling.

3.4. Quaternary structures of unfolded constructs

As representative of the behaviour of the various constructs, the longest (FL) and shortest (239Δ) constructs were subjected to temperatures below, in the middle, and above the transitions in order to ascertain whether the tetrameric forms of the channels stayed intact during the thermal denaturation processes. This was assayed by their profiles on calibrated size exclusion chromatography (Supplemental Fig. 1). The FL sample at 25°C (below the transition) produced a single peak corresponding to tetramer. Mid-transition, a small amount of higher molecular weight material (aggregate) was visible, and at temperatures above the denaturation transition, more aggregate was present. This aggregate is the reason that the denaturation processes were not reversible, and hence why it was not possible to calculate thermodynamic parameters for the transitions. However, in none of the samples was any monomeric protein visible. The shortest sample (239Δ), which did not include any of the CTD residues, was also exclusively tetrameric at the lowest temperature, and the tetramer was the dominant peak at the other temperatures as well. Whilst at elevated temperatures, a small amount of aggregate was present, again no monomer was detectable at any temperature.

These studies clearly indicate that the transitions observed did not result from the destabilization of the tetrameric channels, but rather were due to changes in secondary structure as the proteins unfolded.

3.5. Partial unfolding and refolding

To explore the initial part of the unfolding process which occurs below 40 °C, the longest and shortest constructs were partially unfolded by raising the temperature from 20° to 40 °C, and then cooling again to 20 °C (Fig. 7). The shortest construct (239Δ) did not undergo substantial change over this temperature range, but whatever small change did occur was reversible, resulting in a refolded protein (Fig. 7(b), Table 2). In contrast, the FL protein exhibited a substantially larger change (Fig. 7(a), Table 2), and that change was not reversible upon cooling. This suggests that the initial irreversible step in the thermal unfolding of the intact protein was the consequence of changes to the CTD residues, rather than the TM residues. The likely source of such an irreversible unfolding is the distal region of the CTD which is helical and has been proposed to form a four helix coiled-coil structure in the tetramer. If the unfolding of the helical residues leads to the unravelling of the

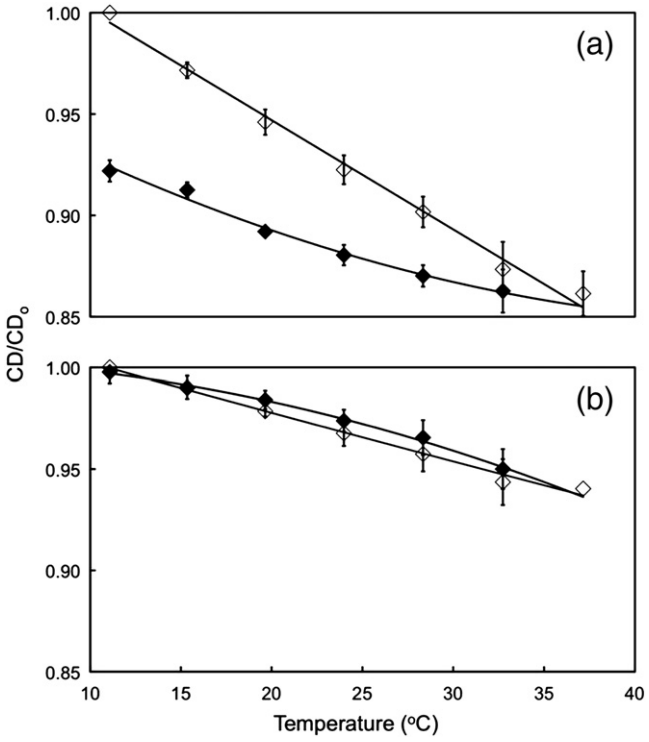

Fig. 7. Partial unfolding and refolding plots for (a) FL and (b) 239Δ constructs derived from plotting the normalized magnitude of the peak at 209 nm as a function of temperature during heating (○) heating and cooling (●). The error bars represent 1 standard deviation in the measurements between replicate experiments.

coiled-coil motif, it is topologically unlikely that this super-secondary structure will reform upon cooling. In contrast, the short construct does not possess a coiled-coil and hence is not prevented from proper refolding.

4. Discussion

4.1. NaChBac has a predominantly helical secondary structure

NaChBac is a multi-pass integral membrane protein with 6 TM segments that are essentially entirely helical, and an extramembranous CTD which has both helical and unordered regions. Its net helical secondary structures calculated based on SRCD data in two different detergents, Cymal-5 (this study) and dodecyl maltoside [37], were 66 and 67%, respectively. These values are very similar to each other and also to the calculated helical secondary structure (68%) of another bacterial sodium channel homologue, NavAb whose crystal structure was recently determined in a lipid environment [31]. This is despite the two homologues having only 37% sequence identity. These close correspondences are an indication of the accuracy of the SRCD method for secondary structure determination.

Table 2
Partial unfolding and refolding of the longest and shortest constructs.

Construct	%H 20	%H 40	%H 40->20	#unfolded	#refolded
FL	66 ± 2	59 ± 1	59 ± 1	19	0
239Δ	67 ± 2	66 ± 1	67 ± 2	2	2

%H 20 is the % of residues that are helical at 20° C; %H 40->20 is the % of residues that are helical after cooling from 40° to 20 °C.
#unfolded is the number of residues unfolded at 40 °C; #refolded is the number of residues unfolded after cooling from 40° to 20 °C.

4.2. NaChBac is resistant to thermal unfolding

Like many other membrane proteins, FL NaChBac retains substantial amounts of regular secondary structure after heating to high temperature. Even at temperatures above 75 °C, it retained a significant helical content (>40%). Previous studies with other helical membrane proteins [4,8,16,40,41], have found that unlike soluble proteins, following either extensive thermal or chemical denaturation they tend to retain on the order of half (or more) of their original helical content. This suggests that either helical secondary structures are generally highly resistant to unfolding, or that the TM regions (which are mostly helical) are more resistant to unfolding than are the EM regions. To date, few studies have been able to distinguish between these two possibilities.

4.3. The EM and TM domains of NaChBac differ in their thermal lability

The aim was to define the structure and stability of the EM and TM domains *when part of an intact protein*, hence this study examined the differences between protein constructs with and without the CTD present, rather than examining small isolated peptides corresponding to the C-terminus alone.

In order to determine whether the thermally-resistant regions of the protein arise specifically as a result of their physical localisation in the EM or TM regions, or whether they are merely a result of their being helical, the thermal stabilities of a series of C-terminally truncated NaChBac proteins were compared. Because the C-terminus of this protein is both helical and located in the EM domain, the two possibilities could be distinguished. As the EM CTD was removed, the proportion of thermally-resistant residues increased, indicating that the TM residues are more thermally-stable than the EM ones, even if the latter are located in helical secondary structures. For the most part the TM residues were not thermally labile and retained their helical character even at very elevated temperatures. Indeed the constructs without the CTD retained around 80% of their original helix content. This may be due to either an indirect protective effect of the surrounding amphiphiles, or the more direct effect of the strengths of intramolecular hydrogen bonds in a hydrophobic environment [42]. The observation that the TM residues are highly resistant to thermal denaturation is consistent with a previous study using a designed synthetic entirely transmembrane peptide, where no thermal unfolding of its secondary structure was detected at all [43]. The advantage of the present study is that it utilised a native multipass transmembrane protein, so that both TM and EM effects could be seen in a single species.

4.4. The unfolding pathway of NaChBac involves both reversible and irreversible steps

Taken together the results in this study suggest that the process of thermal unfolding of NaChBac involves an initial unfolding of the very labile EM helical region, a process which untangles the CTD coiled-coil and which is irreversible; this is then followed by the (mostly) reversible unfolding of a very small number of the TM helical residues. Because the main (irreversible) unfolding process (in terms of temperature and number of residues involved) is very similar for the constructs with and without their CTD, this suggests that essentially the TM and EM domains behave as independent entities in terms of thermal unfolding.

What we cannot determine in the present study is which residues in the TM region are the more labile ones. One possible explanation for the susceptibility of a subpopulation of ~30 TM residues to unfolding could be that if the ends of each of the TM helices are less stable than the intervening middle sections, then a few helical residues at the end of each TMS could “unravel” at the highest temperatures. However, the sequences of most of the TM segments are predicted

to have either N- or C-caps (Supplementary Fig. 2), which would suggest the ends of the helices may be relatively stable [44,45], making this explanation less likely. An alternative possibility is that one of helices (the number of residues lost would suggest one helix) completely unfolds. Again based on the capping argument, this would suggest that TM4, the voltage sensor which appears to be mobile in the functional cycle, would be the most susceptible (and likely) one. However, although these bioinformatics arguments are suggestive, we cannot discern between these two possibilities experimentally.

5. Conclusions

In summary, this study has been able to dissect the different contributions and roles of the TM and EM residues in the process of thermal denaturation of an integral multipass membrane protein.

Acknowledgements

This work was supported by grants to BAW from the U.K. Engineering and Physical Sciences Research Council (EPSRC), the U.K. Biotechnology and Biological Sciences Research Council (BBSRC) and the Heptagon Fund, and a Wellcome Trust VIP grant to the Department of Crystallography. SRCD beamtime was provided by grants (to BAW) from the Institute for Synchrotron Facilities (ISA), Denmark and the Beijing Synchrotron Radiation Facility (BSRF), China, and the Soleil Synchrotron, France. Access to ISA is acknowledged under the EU Integrated Infrastructure Initiative (I3), Integrated Activity on Synchrotron and Free Electron Laser Science (IA-SFS), contract number RII3-CT-2004-506008. We thank Dr. R.W. Janes of Queen Mary, University of London for help with SRCD data collection.

Appendix A. Supplementary data

Supplementary data to this article can be found online at doi:10.1016/j.bbamem.2011.12.019.

References

[1] K.A. Dill, S.B. Ozkan, T.R. Weikl, J.D. Chodera, V.A. Voelz, The protein folding problem: when will it be solved? Curr. Opin. Struct. Biol. 17 (2007) 342–346.
[2] R.D. Schaeffer, V. Daggett, Protein folds and protein folding, Protein Eng. Des. Sel. 1–2 (2011) 11–19.
[3] P.J. Booth, P. Curnow, Membrane proteins shape up: understanding in vitro folding, Curr. Opin. Struct. Biol. 16 (2006) 480–488.
[4] C.G. Brouillette, D.D. Muccio, T.K. Finney, pH dependence of bacteriorhodopsin thermal unfolding, Biochemistry 26 (1987) 7431–7438.
[5] A.O. O'Reilly, K. Charalambous, G. Nurani, A.M. Powl, B.A. Wallace, G219S mutagenesis as a means of stabilizing conformational flexibility in the bacterial sodium channel NaChBac, Mol. Membr. Biol. 25 (2008) 670–676.
[6] P.J. Booth, R.H. Templer, W. Meijberg, S.J. Allen, A.R. Curran, M. Lorch, In vitro studies of membrane protein folding, Crit. Rev. Biochem. Mol. Biol. 36 (2001) 501–603.
[7] S.A. Contera, V. Lemaître, M.R. de Planque, A. Watts, J.F. Ryan, Unfolding and extraction of a transmembrane alpha-helical peptide: dynamic force spectroscopy and molecular dynamics simulations, Biophys. J. 89 (2005) 3129–3140.
[8] A. Dutta, K.C. Tirupula, U. Alexiev, J. Klein-Seetharaman, Characterization of membrane protein non-native states. 1. Extent of unfolding and aggregation of rhodopsin in the presence of chemical denaturants, Biochemistry 49 (2010) 6317–6328.
[9] F.N. Barrera, M.L. Renart, M.L. Molina, J.A. Poveda, J.A. Encinar, A.M. Fernández, J.L. Neira, J.M. González-Ros, Unfolding and refolding in vitro of a tetrameric, alpha-helical membrane protein: the prokaryotic potassium channel KcsA, Biochemistry 44 (2005) 14344–14352.
[10] N.J. Brooks, O. Ces, R.H. Templer, J.M. Seddon, Pressure effects on lipid membrane structure and dynamics, Chem. Phys. Lipids 164 (2011) 89–98.
[11] D.J. Müller, A. Engel, Atomic force microscopy and spectroscopy of native membrane proteins, Nat. Protoc. 2 (2007) 2191–2197.
[12] J.U. Bowie, Membrane proteins: a new method enters the fold, Proc. Natl. Acad. Sci. U. S. A. 101 (2004) 3995–3996.
[13] E. van den Brink-van der Laan, V. Chupin, J.A. Killian, B. de Kruijff, Stability of KcsA tetramer depends on membrane lateral pressure, Biochemistry 43 (2004) 4240–4250.
[14] R. Renthal, An unfolding story of helical transmembrane proteins, Biochemistry 45 (2006) 14559–14566.
[15] J.L. Eisele, J.P. Rosenbusch, In vitro folding and oligomerization of a membrane protein. Transition of bacterial porin from random coil to native conformation, J. Biol. Chem. 265 (1990) 10217–10220.
[16] T. Haltia, E. Freire, Forces and factors that contribute to the structural stability of membrane proteins, Biochim. Biophys. Acta 1241 (1995) 295–322.
[17] P. Curnow, P.J. Booth, Combined kinetic and thermodynamic analysis of alpha-helical membrane protein unfolding, Proc. Natl. Acad. Sci. U. S. A. 104 (2007) 18970–18975.
[18] J.P. Schlebach, M.S. Kim, N.H. Joh, J.U. Bowie, C. Park, Probing membrane protein unfolding with pulse proteolysis, J. Mol. Biol. 406 (2011) 545–551.
[19] F.W. Lau, J.U. Bowie, A method for assessing the stability of a membrane protein, Biochemistry 36 (1997) 5884–5892.
[20] K. Charalambous, B.A. Wallace, NaChBac: the long lost sodium channel ancestor, Biochemistry 50 (2011) 6742–6752.
[21] K. Mio, M. Mio, F. Arisaka, M. Sato, C. Sato, The C-terminal coiled-coil of the bacterial voltage-gated sodium channel NaChBac is not essential for tetramer formation, but stabilizes subunit-to-subunit interactions, Prog. Biophys. Mol. Biol. 103 (2010) 111–121.
[22] A.M. Powl, A.O. O'Reilly, A.J. Miles, B.A. Wallace, Synchrotron radiation circular dichroism spectroscopy-defined structure of the C-terminal domain of NaChBac and its role in channel assembly, Proc. Natl. Acad. Sci. U. S. A. 107 (2010) 14064–14069.
[23] E. Gasteiger, C. Hoogland, A. Gattiker, S. Duvaud, M.R. Wilkins, R.D. Appel, A. Bairoch, Protein identification and analysis tools on the ExPASy server, in: J.M. Walker (Ed.), The Proteomics Protocols Handbook, Humana Press, 2005, pp. 571–609.
[24] J.G. Lees, B.R. Smith, F. Wien, A.J. Miles, B.A. Wallace, CDtool-an integrated software package for circular dichroism spectroscopic data processing, analysis, and archiving, Anal. Biochem. 332 (2004) 285–289.
[25] L. Whitmore, B.A. Wallace, Protein secondary structure analyses from circular dichroism spectroscopy: methods and reference databases, Biopolymers 89 (2008) 392–400.
[26] S.W. Provencher, J. Glockner, Estimation of globular protein secondary structure from circular dichroism, Biochemistry 20 (1981) 33–37.
[27] I.H. van Stokkum, H.J. Spoelder, M. Bloemendal, R. van Grondelle, F.C. Groen, Estimation of protein secondary structure and error analysis from circular dichroism spectra, Anal. Biochem. 191 (1990) 110–118.
[28] N. Sreerama, R.W. Woody, Estimation of protein secondary structure from circular dichroism spectra: comparison of CONTIN, SELCON, and CDSSTR methods with an expanded reference set, Anal. Biochem. 287 (2000) 252–260.
[29] J.G. Lees, A.J. Miles, F. Wien, B.A. Wallace, A reference database for circular dichroism spectroscopy covering fold and secondary structure space, Bioinformatics 22 (2006) 1955–1962.
[30] J.P. Hennessey Jr., W.C. Johnson Jr., Information content in the circular dichroism of proteins, Biochemistry 20 (1981) 1085–1094.
[31] J. Payandeh, T. Scheuer, N. Zheng, W.A. Catterall, The crystal structure of a voltage-gated sodium channel, Nature 457 (2011) 353–358.
[32] W. Kabsch, C. Sander, Dictionary of protein secondary structure: pattern recognition of hydrogen-bonded and geometrical features, Biopolymers 22 (1983) 2577–2637.
[33] D.P. Klose, B.A. Wallace, R.W. Janes, 2Struc: the secondary structure server, Bioinformatics 26 (2010) 2624–2625.
[34] L. Whitmore, B. Woollett, A.J. Miles, D.P. Klose, R.W. Janes, B.A. Wallace, PCDDB: the Protein Circular Dichroism Data Bank, a repository for circular dichroism spectral and metadata, Nucleic Acids Res. 39 (2011) D480–D486.
[35] S. Uysal, V. Vasquez, V. Tereshko, K. Esaki, F.A. Fellouse, S.S. Sidhu, S. Koide, E. Perozo, A. Kossiakoff, Crystal structure of full-length KcsA in its closed conformation, Proc. Natl. Acad. Sci. U. S. A. 106 (2009) 6644–6649.
[36] B.A. Wallace, Protein characterisation by synchrotron radiation circular dichroism spectroscopy, Q. Rev. Biophys. 42 (2009) 317–370.
[37] G. Nurani, M. Radford, K. Charalambous, A.O. O'Reilly, N.B. Cronin, S. Haque, B.A. Wallace, Tetrameric bacterial sodium channels: characterization of structure, stability, and drug binding, Biochemistry 47 (2008) 8114–8121.
[38] E.C. McCusker, N. D'Avanzo, C.G. Nichols, B.A. Wallace, A simplified bacterial "Pore" provides insight into the assembly, stability and structure of sodium channels, J. Biol. Chem. 286 (2011) 16386–16391.
[39] K. Charalambous, A.O. O'Reilly, P.A. Bullough, B.A. Wallace, Thermal and chemical unfolding and refolding of a eukaryotic sodium channel, Biochim. Biophys. Acta 1788 (2009) 1279–1286.
[40] K. Oikawa, D.M. Lieberman, R.A. Reithmeier, Conformation and stability of the anion transport protein of human erythrocyte membranes, Biochemistry 24 (1985) 2843–2848.
[41] I. Protasevich, Z. Yang, C. Wang, S. Atwell, X. Zhao, S. Emtage, D. Wetmore, J.F. Hunt, C.G. Brouillette, Thermal unfolding studies show the disease causing F508del mutation in CFTR thermodynamically destabilizes nucleotide-binding domain 1, Protein Sci. 19 (2010) 1917–1931.
[42] N. Ben-Tal, A. Ben-Shaul, A. Nicholls, B. Honig, Free-energy determinants of a-helix insertion into lipid bilayers, Biophys. J. 70 (1996) 1803–1812.
[43] M.B. Ulmschneider, J.P. Doux, J.A. Killian, J.C. Smith, J.P. Ulmschneider, Mechanism and kinetics of peptide partitioning into membranes from all-atom simulations of thermostable peptides, J. Am. Chem. Soc. 132 (2010) 3452–3460.
[44] L.G. Presta, G.D. Rose, Helix signals in proteins, Science 240 (1988) 1632–1641.
[45] J.S. Richardson, D.C. Richardson, Amino acid preferences for specific locations at the ends of alpha helices, Science 240 (1988) 1648–1652.